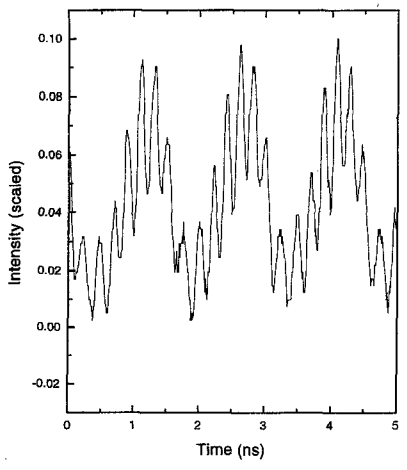

CTuM4 Fig. 3. A fragment of the pulse of *p*-Ge laser with a silicon spacer in the cavity. $B = 0.44\ T$, $E = 0.57$ kV/cm.

phase distribution and appears different for each laser shot.

Another cavity is formed by including a 8.4 mm Si spacer between the *p*-Ge crystal and the back mirror (see Fig. 3). The calculated full round-trip time is $\tau_2 = 2(n_{Ge}L_{Ge} + n_{Si}L_{Si}/c \simeq 1505$ ps. The period of fast oscillations, caused by reflections from the Ge/Si boundary, is $\tau_3 \simeq 215$ ps, which differs somewhat from the calculated Si spacer round-trip time $\tau_{3'} = 2n_{Si}L_{Si}/c \simeq 190$ ps. This could be interpreted as an effect of frequency pulling of the added cavity by the main cavity, where the observed oscillation frequency is defined by a harmonic of the main cavity round-trip frequency, so that $\tau_3(215\text{ ps}) = \tau_2(1505\text{ ps})/k$, where k is an integer (here $k = 7$). Thus, the eigenmodes of the coupled laser cavity are still defined by the main resonator in spite of the reflections from the Ge/Si boundary. Fourier transform of the data reveals additional weaker harmonics at $k = 6$, 8, and 9. Note, that the closest integer expected from the calculated round trips is 8 ($\simeq \tau_2/\tau_3'$).

The effect is important for the development of passive or active mode locking of the *p*-Ge laser with coupled cavities, where a saturable absorber or gain modulator may be inserted inside the *p*-Ge laser cavity. Despite intrinsic reflections caused by the added spacer inside the laser cavity, a train of short pulses on a harmonic of the main cavity round-trip frequency can be generated.

This work is supported by NSF and AFOSR/BMDO. Co-authors from IPM thank the Russian Foundation for Basic Research (grants 96-02-19275, 96-02-00249 G) for support of this work.

**Institute for Physics of Microstructures, Russian Academy of Sciences, GSP-105, Nizhny Novgorod 603600, Russia*

1. E. Gornik and A.A. Andronov, eds., "Special Issue Far-infrared Semiconductor Lasers," Opt. Quantum Electron. **23,** (1991).
2. J.N. Hovenier, A.V. Muravjov, S.G. Pavlov, V.N. Shastin, R.C. Strijbos, W.Th. Wenckebach, Appl. Phys. Lett. **71,** 443–445 (1997).
3. A.V. Bespalov, Appl. Phys. Lett. **66,** 2703–2705 (1995).

CTuM5

Comparison of different methods of locking a tunable diode laser to iodine transitions for applications in interferometry

F. Imkenberg, J. Lazar,* A. Abou-Zeid,
Physikalisch-Technische Bundesanstalt, Bundesallee 100, D-38116 Braunschweig, Germany; E-mail: Frank.Imkenberg@PTB.de

With the aim of increasing the coherence length of 633-nm laser diodes and realizing a large tuning range, an external-cavity diode laser (ECL) in the Littman design was set up.[1,2] The front facet of the laser diode was antireflection coated and the light from the diode is reflected back via a fixed grating and a rotatable mirror. The temperature of the external cavity and the laser diode is stabilized by one controller using Peltier-elements. We set up a highly stable and low noise current source[3] and added a fast current control.[4]

The best results were achieved with a laser diode of the type SDL-7501-G1, which has an output power of 15 mW at a wavelength of $\lambda = 635$ nm before antireflection coating. With the ECL a maximum optical output power of >8 mW was achieved. The tuning range is typically lager than 16 nm. Within a range of more than 1 nm the laser can be tuned without any mode hops. Due to the stable mechanical design of the external cavity the linewidth is reduced to <500 kHz for 100 ms integration time, compared to more than 100 MHz for the uncoated solitary laser diode. In the modehop-free tuning range of the ECL more than 20 strong Doppler-broadened absorption lines were detected, which are suitable as reference for frequency locking by means of a simple differential spectroscopy (Fig. 1). With the ECL locked to a flank of the P(33)6-3 line at 632.990 nm a stability better than $\Delta\nu/\nu = 5 \times 10^{-8}$ was achieved for sampling time intervals larger than 0.5 s.

For applications where higher frequency stability is needed a Doppler-free saturation spectroscopy technique and frequency-modulation spectroscopy (FMS) were used.[5] The ECL allows fast frequency tuning by the diode current and slow but wideband tuning by rotating of the mirror. The FMS with its high-frequency modulation and detection allows us to establish a fast current-controlling servo-loop resulting in even more significant line-narrowing. In the setup for FMS (Fig. 2) a 500-mm-long iodine cell is used, the sidebands are generated in an electro-optic modulator (EOM) with a spacing of 10 MHz from the carrier. To eliminate the Doppler background

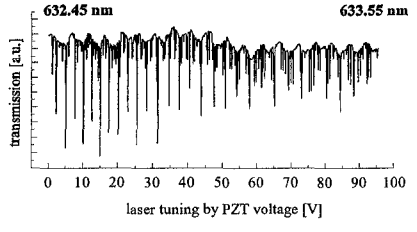

CTuM5 Fig. 1. Doppler-broadened absorption lines of molecule iodine within the modehop-free tuning range of the ECL.

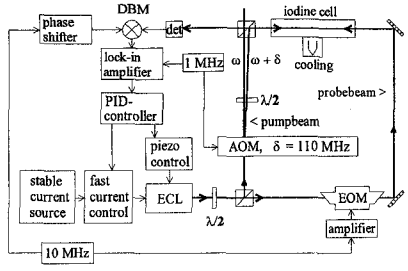

CTuM5 Fig. 2. Setup for Doppler-free FMS and frequency stabilization of the ECL.

and however achieve a large bandwidth of the feedback loop, we realized a fast analog lock-in amplifier and used an acousto-optic modulator (AOM) with a blanking frequency of 1 MHz.

The achieveable frequency stability is better than 10^{-10} for integration times larger than 0.5 s. This is a first preliminary result. Optimization of the servo loop and international frequency comparisons will lead to an improvement of the reproducibility and uncertainty.

**Institute of Scientific Instruments, Academy of Sciences of the Czech Republic, Královopolská 147, 612 64 Brno, Czech Republic*

1. K. Liu and M.G. Littman, Opt. Lett. **6,** 117–118 (1981)
2. P. McNicholl and H.J. Metcalf, Appl. Opt. **24,** 2757–2761 (1985),
3. K.G. Liebbrecht and J.L. Hall, Rev. Sci. Instrum. **64,** 2133–2135 (1993)
4. H.R. Telle, Spectrochim. Acta Rev. **15,** 301–327 (1993).
5. G.C. Bjorklund and M.D. Levenson, Phys. Rev. A **24,** 166–169 (1981).

CTuM6

Improve output beam quality using new-type flared semiconductor laser amplifiers

Ching-Fuh Lin, Jie-Wei Lai, Yu-Jia Chang,
Institute of Electro-Optical Engineering, and Department of Electrical Engineering, National Taiwan University, Taipei, Taiwan, R.O.C.; E-mail: cflin@cc.ee.ntu.edu.tw

A reliable, coherent, and high-power laser source is important for many applications. High-power semiconductor lasers therefore draw much attention due to their compactness, low cost, and other advantages. Recently flared semiconductor laser amplifiers have demonstrated the highest output power with extremely good spatial coherence.[1,2] However, filamentation is still formed when such devices are operated at a much higher power level. The physics of the filamentation has been widely studied and mainly attributed to the interaction between the light intensity and the carriers.[3,4] The fluctuation of beam intensity and the variation of the carrier concentration mutually influences one another, leading to the filamentation. However, what is the first cause of the spatial variation remains unexplained.

In this work, we assert that the fluctuation mainly results from the reflection of the light from the boundary of the waveguide. From

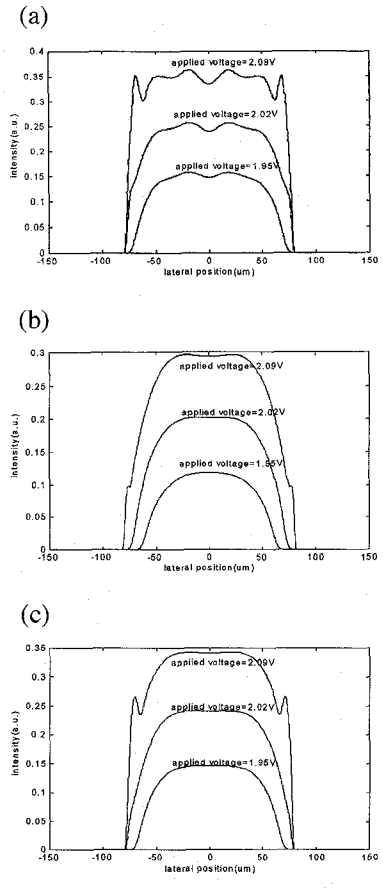

CTuM6 Fig. 1. The output beam profiles: (a) linearly tapered amplifier with 7-μm input aperture; (b) hyperbolically flared amplifier with 7 μm input aperture; (c) linearly tapered amplifier with 1-μm input aperture.

this point of view, the near field of the beam should be improved if the reflection is reduced. This can be achieved as the wave front of the propagation beam is normal to the waveguide boundary. Therefore, we propose that a flared waveguide with a very narrow input and a hyperbolically flared amplifier both could significantly improve the beam quality. The narrow input behaves like a point source, while the hyperbolically flared structure analogizes the expansion of a Gaussian beam.

The theoretical model used to analyze the beam amplification includes both the rate equations of the quantum well structure and the wave equation. This model has taken into account the phenomena involved in the rate equation, optically induced refractive-index change, paraxial beam propagation, nonuniform voltage distribution, current spreading, thermal effect, ohmic heat, photon cooling, and spontaneous emission. The finite-difference vector beam propagation method (FD-VBPM) is used for the simulation. The same simulation has been applied to the conventional tapered semiconductor laser amplifiers and has successfully predicted the filamentation observed previously.

Simulation using the detailed model shows that the near-field beam quality is greatly improved using these new types of amplifiers. Figs. 1(a)–1(c), respectively, show the output beam profiles for three types of amplifiers: linearly tapered, hyperbolically flared, and narrow-input ones. All of the input powers are 10 mW. The output end of the waveguides is 160 μm wide. The input apertures are 7 μm for the linearly tapered and hyperbolically flared amplifiers and 1 μm for the narrow-input one. The simulated L-I and I-V characteristics of the three types amplifiers are very similar. However, the simulation results show that both the hyperbolically flared and the narrow-input amplifiers could significantly reduce the filaments because the expansion of the beam matches the shapes of these waveguides better. Detailed discussions will be given in the presentation.

1. D.F. Welch, R. Parke, D. Mehuys, A. Hardy, R. Lang, S. O'Brien, S. Scifres, Electron. Lett. **28,** 2011–2013 (1992).
2. D. Mehuys, S. O'Brien, R.J. Lang, A. Hardy, D.F. Welch, Electron. Lett. **30,** 1855–1856 (1993).
3. J.R. Marciante and G.P. Agrawal, IEEE J. Quantum Electron. **32,** 590–596 (1996).
4. Zheng Dai and Peter Unger, in *Digest of CLEO/Europe'96* (Optical Society of America, Washington, D.C., 1996), paper CThI30.

CTuM7

Single-longitudinal-mode, nonantireflection-coated, fiber grating laser with a 50-dB side-mode suppression ratio

Z. Frank Fan, J.H. Song, Peter J.S. Heim, S.H. Cho, Mario Dagenais, F.G. Johnson,* P. Sivanesan,** James Sirkis,** *Department of Electrical Engineering and Joint Program for Advanced Electronic Materials, University of Maryland, College Park, Maryland 20742; E-mail: dage@glue.umd.edu*

Butt-coupled fiber grating lasers (FGLs)[1–3] can be viable alternatives to conventional external-cavity semiconductor lasers (ECSLs) or distributed feedback lasers because they can provide narrow-linewidth, stable single-mode lasing, and are of small size, low chirp, and less costly. In order to achieve the demanding single-mode lasing characteristics and high dynamic range required in many applications, such as characterization of erbium-doped fiber amplifiers (EDFAs), laser radar, and environmental monitoring, it is essential to reduce the reflectivity of both the laser diode facet and the fiber grating end facing the laser diode to suppress the resulting Fabry–Perot resonances. Traditionally, antireflection (AR) coatings are deposited on both the laser diode facet and the fiber end.[3,4] This makes the manufacturing process complicated and adversely contribute to the cost and the reliability of such lasers. Here we report on a butt-coupled 1.55-μm FGL with no AR coating on either the laser facet or the fiber end. Stable single-longitudinal-mode operation with a 50-dB side-mode suppression ratio is demonstrated.

The structure of the FGL is shown in Fig. 1. A single-angled-facet (SAF) laser diode was used as the gain medium. The SAF laser diode is an InGaAsP/InP four quantum well ridge-waveguide device described previously in Ref. 5. The waveguide traverses an arc along the 1 mm length of the device, with a constant radius of curvature of about 9.5 mm, intersecting the facet cleavage plane at normal incident on one side and at 6° relative to the facet normal on the other side. The normal side has a reflectivity of 33% and acts as the output facet. The modal reflectivity of the angled facet was measured to be approximately $R = 2 \times 10^{-5}$.

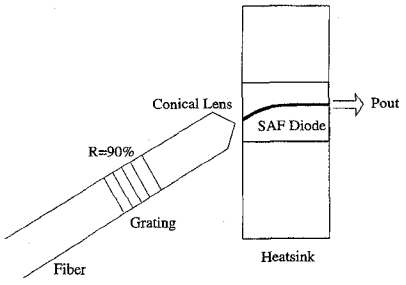

CTuM7 Fig. 1. Schematic diagram of the butt-coupled fiber grating laser.

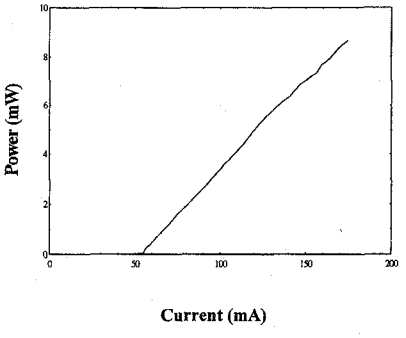

CTuM7 Fig. 2. L-I curve of the FGL.

A fiber Bragg grating was written in a H_2-loaded single-mode fiber (Corning SMF28) using the phasemask method.[6] The total grating length was 10 mm with the beginning of the grating located 10 mm away from the fiber end. The grating has a reflectivity of 90% at the center wavelength of 1549 nm with a 3-dB bandwidth of 0.2 nm. A conical lens with a 140° cone angle provided high coupling efficiency to the laser diode.[7] The conical lens also significantly reduced the back reflection from the fiber end surface to <-50 dB. The fiber grating was fixed in a silica V-groove using UV curable epoxy and then actively aligned to the laser diode.

Figure 2 shows the cw light output versus injection current curve of the FGL. The FGL has a threshold current of 55 mA with output facet slope efficiency of 0.076 mW/mA resulting in approximately 8 mW of output power at a bias current of 160 mA. A side-mode suppression ratio of 50 dB was obtained as shown in Fig. 3 for a bias current of 140 mA. Single-longitudinal-mode operation was confirmed by using a scanning Fabry–Perot interferometer with a free spectral range of 50 GHz, finesse of 500, and a dynamic range of approximately 30 dB. The linewidth of this laser was measured by a delayed self-homodyne method to be less than 150 kHz. Discrete mode hopping to the next external-cavity longitudinal-mode, spaced approximately 9 GHz apart, was